*forests*

MDPI

*Article*

# Impregnation of Medium-Density Fiberboard Residues with Phase Change Materials for Efficient Thermal Energy Storage

**Gustavo E. Rodríguez [1,*], Cecilia Bustos Ávila [1,*], Romina Romero [2] and Alain Cloutier [3]**

[1] Centro de Biomateriales y Nanotecnología, Departmento de Ingeniería en Maderas, Facultad de Ingeniería, Universidad del Bío Bío, Concepcion 4030000, Chile
[2] Departamento de Química Analítica e Inorgánica, Universidad de Concepción, Concepcion 4030000, Chile; rominaromero@udec.cl
[3] Renewable Materials Research Center (CRMR), Department of Wood and Forest Sciences, Université Laval, Quebec, QC G1V 0A6, Canada; alain.cloutier@sbf.ulaval.ca
* Correspondence: gustavo.rodriguez1901@alumnos.ubiobio.cl (G.E.R.); cbustos@ubiobio.cl (C.B.Á.)

**Abstract:** The wood-based panel industry generates a significant amount of solid residues in its production activities, including medium-density fiberboard (MDF) molding manufacturing. These residues consist of fine fibers measuring between 0.15 mm and 1.19 mm in length. A large proportion of them currently needs to be utilized, mainly due to the problem of excessive accumulation. They can be reused as raw material for manufacturing new products by adopting a circular economy approach. Their thermal properties can also be enhanced by impregnating them with phase change materials (PCMs). This research aims to develop a process for impregnating MDF panel residues (R) with PCMs to obtain shape-stabilized compounds capable of storing thermal energy. Three different commercially available PCMs were used. They were incorporated in the MDF residues by vacuum impregnation. The morphology, chemical structure, thermal stability, and phase change properties of the compounds obtained were studied by scanning electron microscopy (SEM), Fourier-transform infrared (FTIR) spectrometry, thermogravimetric analysis (TGA), and differential scanning calorimetry (DSC), respectively. The SEM images indicated the PCM filled the empty spaces in the porous surface of the residue fibers to form shape-stabilized compounds. The FTIR spectrometry results indicated the compounds still exhibited characteristic peaks corresponding to both the MDF residues and the PCMs. No chemical reaction was observed between the two components. Moreover, according to the TGA results, the compounds produced exhibit high thermal stability. The R+PCM1 compound had the highest latent heat capacity of all the compounds developed in this study, reaching a maximum of 57.8 $J \cdot g^{-1}$, and a phase change temperature comparable to that of PCM1. This better thermal performance could be attributed to the compounds having a higher encapsulation ratio (31.4%) than the other compounds developed. Furthermore, the R+PCM1 compound had an absorption capacity of 142.8%. This study, therefore, unveiled a promising alternative for storing thermal energy and valorizing solid MDF residues.

**Keywords:** phase change materials; MDF residues; thermal energy storage; thermal properties

check for updates

**Citation:** Rodríguez, G.E.; Bustos Ávila, C.; Romero, R.; Cloutier, A. Impregnation of Medium-Density Fiberboard Residues with Phase Change Materials for Efficient Thermal Energy Storage. *Forests* **2023**, *14*, 2175. https://doi.org/10.3390/f14112175

Academic Editor: Anuj Kumar

Received: 20 September 2023
Revised: 27 October 2023
Accepted: 30 October 2023
Published: 1 November 2023

**Copyright:** © 2023 by the authors. Licensee MDPI, Basel, Switzerland. This article is an open access article distributed under the terms and conditions of the Creative Commons Attribution (CC BY) license (https://creativecommons.org/licenses/by/4.0/).

## 1. Introduction

In recent years, the wood-based panel industry has undergone significant technological, production-related, and commercial advancements to provide a wide range of products that can effectively replace solid wood in some applications. According to data from the Food and Agriculture Organization of the United Nations (FAO), between the early 1960s and 2015, global wood-based panel production increased from 26 million $m^3$ to 387.7 million $m^3$ [1]. In Chile, the industrial production of wood-based panels and veneers reached 3.6 million $m^3$ in 2021, which reflects an average annual rate of 8.1% over the past 35 years [2]. The manufacturing of moldings from medium-density fiberboard (MDF)

panels is a particularly significant source of MDF residues. These residues consist mainly of wood fiberssmaller in size (0.15–1.19 mm in length) than those used in MDF panel production. Some of these residues are utilized for power generation in the wood-based panel industry. A very small fraction of them serves as filler material for new panels. Nevertheless, most residues are stockpiled in mill yards and eventually buried. Considering the increase in Chilean panel and molding production, the substantial amount of wood residues consequently generated must be acknowledged. These residues, and the residues produced by the sawmill sector in general, present a significant challenge for the industry, as they accumulate in large volumes to be effectively dealt with. For example, in 2021, the Chilean sawmill industry generated a staggering 5.4 million $m^3$ of wood residues, including bark, chips, sawdust, and shavings [3]. In the European Union, a zero-waste program has been implemented aiming to reduce the use of virgin raw materials. A reduction of around 25% is estimated for the year 2030, with the ultimate target being to reduce greenhouse gas production by 40%. One of the most relevant ways of doing so is to use wood residues as bio-insulation in housing [4].

Considering there is a growing need to optimize resource utilization in the wood-based panel industry, more and more researchers are exploring alternative methods of adding value to MDF residues. One possible approach involves developing materials capable of storing solar thermal energy. Phase change materials (PCMs) are crucial for energy storage as they can absorb, store, and release thermal energy through endothermic and exothermic processes [5–7]. Thermal energy is stored when a PCM melts and is released when it solidifies [8–10]. PCMs can be classified as organic, for example, paraffin and fatty acids, or inorganic, such as hydrated salts [11]. Organic PCMs have gained significant research attention because they are less corrosive than inorganic ones, and do not experience supercooling issues [12]. Another classification of PCMs includes eutectic mixtures, which consist of two or more chemical components that can change phase together [11]. These mixtures are characterized by their non-toxic nature, excellent thermal stability, and high phase change enthalpy (or latent heat) [13]. The main advantage of using PCMs for thermal energy storage is they make use of one of the most abundant types of renewable energy: solar energy. It is possible, for example, to store excess heat in buildings and release it when the indoor temperature is lower. This concept would help to reduce the amount of energy homes consume to operate heating and cooling systems. Incorporating PCMs in building structures for thermal energy storage would serve to mitigate energy intermittency. It would therefore help to keep the indoor temperature consistent and effectively regulate temperature fluctuations.

PCMs have been successfully incorporated in a variety of building materials, such as gypsum [14–17], brick [18–20], and cement [21–24]. However, it is important to mention one of the main challenges researchers have faced: PCM loss during phase transition. Using wood as a support matrix can help to mitigate this issue since the wood's porosity supports the formation of an internal network between the PCM and its constituent elements to produce a shape-stable material. Moreover, Meng et al. [25] developed a stable compound using polyethylene glycol (PEG) as the PCM and balsa wood that had previously undergone a delignification process to enhance PCM incorporation. Their results showed a high encapsulation capacity (83.5%) with minimal loss during phase change. The amount of latent heat obtained in this study is ten times greater than the amount reported by Frazzica et al. [26], who incorporated PCM in cement, and about seven times greater than the amount recorded by Yaras et al. [14], who developed a gypsum-PCM compound. It is important to note the compound's heat storage capacity is dependent on the thermal attributes of the PCM used. However, impregnating wood has been shown to provide better performance than cement or gypsum. Similarly, Ma et al. [27] conducted a study in which delignified and non-delignified wood slices were impregnated with a mixture of capric and palmitic acids. Their results indicated the wood pores were effectively filled with PCM and a physical bond had been formed without any chemical bond formation between the components, as confirmed by FTIR spectrometry analysis. Other researchers

have focused on incorporating PCMs in wood flour rather than wood slices. Cheng and Feng [28] developed a stable compound using delignified poplar wood flour and myristic alcohol as the PCM. They performed a leakage test, which revealed no material loss after 30 min of heating at 80 °C and therefore excellent thermal stability. Jiang et al. [29] prepared stable compounds by combining PEG and wood flour using a direct impregnation method. Their results showed the compound exhibited good thermal stability, with decomposition occurring above 200 °C. They achieved a 52.8% impregnation rate for PEG in the substrate used and a maximum latent heat of 90.9 $J \cdot g^{-1}$. Sari et al. [30] used a similar methodology and impregnated wood fibers with a mixture of capric and stearic acids. Their results showed the fibers were successful impregnated with the eutectic PCM and the compound achieved a maximum latent heat of 92.1 $J \cdot g^{-1}$. The thermal properties of the compound developed remained stable after thermal cycling.

To our knowledge, there is no published literature reporting the impregnation of PCMs in MDF residues to produce a compound material with improved thermal properties. The above context provides an opportunity to valorize the MDF residues generated in the MDF molding industry. This novel study aims to develop a process to impregnate MDF residues with PCMs to obtain shape-stabilized compounds suitable for thermal energy storage.

## 2. Materials and Methods

### 2.1. Materials

Solid residues (R) generated during the production of moldings from *Pinus radiata* MDF panels in the Bío Bío region of Chile were used. Both pre-screened and unscreened residues were analyzed. These residues, which looked like dust flour, consisted of small fibers measuring 0.15–1.19 mm in length and originated from MDF panels manufactured using urea-formaldehyde (UF) adhesive with a solid content of 65% and a resin content of 14%. The pressing temperature was 240 °C. Since the residues were a by-product of the MDF panels, they contained small particles of UF adhesive. This means there were fewer voids in the wood fibers to impregnate with other materials. However, as demonstrated below, it was possible to impregnate them with PCMs. The MDF residues were morphologically characterized by granulometric analysis and chemically characterized following different standards detailed below. Unscreened residues were selected and dried in an oven for 4 h at 103 ± 2 °C until their moisture content reached 4% before being used [31]. The PCMs used in this study include the bio-based material PureTemp 15X (PCM1), which is produced from agricultural sources and has a phase change temperature close to 15 °C, and two petroleum-derived materials, Rubitherm RT12 (PCM2) and Rubitherm RT15 (PCM3), which have a phase change temperature close to 12 °C and 15 °C, respectively. Before impregnation, the PCMs were analyzed to determine their water content using the Karl-Fisher method with a solution of iodine in methanol and pyridine as a water-sequestering agent. PCM1′s water content was 0.035 ± 0.001%, while PCM2′s and PCM3′s were below the detection threshold.

#### Granulometric and Chemical Analysis of MDF Residues

Granulometric and chemical analyses were conducted on the MDF residues. For granulometric characterization, a representative sample of 300 g was taken, and the analysis was replicated 5 times. The size distribution of the fibers of both pre-screened and unscreened residues was determined and compared to that of the fibers used to produce the MDF panels. A Fritsch laborgerätebau vibrating sieve (model Industriestr. 8. Birkenfeld, Germany) was utilized for this purpose. The chemical composition of the samples was determined in accordance with TAPPI standard T 280 [32] for extractive content. The holocellulose and alpha-cellulose content were determined in accordance with TAPPI standard T9 wd-75 [33], the lignin content, TAPPI standard T222 om-11 [34], and the ash content, TAPPI standard T211 om-12 [35].

### *2.2. Preparation of the Shape-Stabilized Compounds: MDF Residues and PCM*

The compounds were prepared using a vacuum impregnation method. First, the PCMs were heated in a beaker to 70 °C. Next, the MDF residues were added, and the mixture was continuously stirred for 30 min to ensure the homogenization of both materials. Then, the mixture was placed in a Vacucell-22-Standard blue line vacuum oven (MMM group, München, Germany) at 60, 70, and 80 °C using a vacuum pressure of 0.5 bar. Two different impregnation times (20 and 40 min) were employed, and a residue-to-PCM mass ratio of 1:1 was used throughout. Each combination of PCM (3), temperature (3), and time (2) was an independent treatment (18 different combinations, 5 replicates each). These conditions were defined in preliminary tests and based on the characteristics of the PCMs. The impregnation process used is summarized in Figure 1.

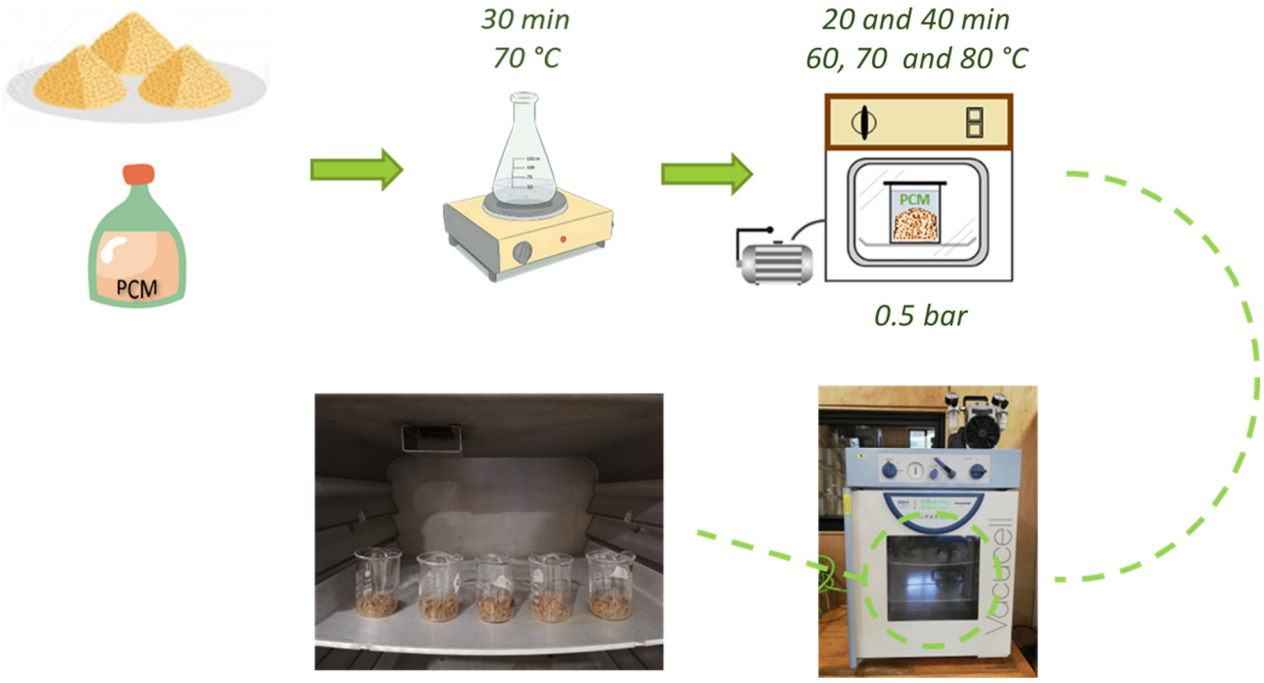



**Figure 1.** Process used to impregnate the MDF residues with PCMs and obtain compounds.

### *2.3. Characterization*

#### 2.3.1. Morphological Characterization

The microstructure and morphology of the MDF residues and the compounds resulting from impregnation with PCMs were examined using a JEOL JSM-6610LV (JEOL, Tokyo, Japan) scanning electron microscope operating at 7 kV. Before observation, the samples were coated with a thin layer of gold for 30 s using a Denton Vacuum sputter. The length, width, and shape of the fibers were measured.

#### 2.3.2. Chemical Structure

The chemical structure of the MDF residues, the PCMs, and the compounds obtained were analyzed using an FTIR spectrometer NICOLET (model Nexus from Thermo Electron Corporation, Carnegie, PA, USA) equipped with a DTGS-KBr detector. The samples were prepared and compressed into pellets using potassium bromide (KBr). The FTIR spectrometer measurements were conducted in the 4000 to 400 $cm^{-1}$ spectral range for analysis. To facilitate accurate spectral comparison, uniform sample quantities were used to prepare the KBr-treated pellets. Data normalization was subsequently performed for a region devoid of any bands of interest.

#### 2.3.3. Thermal Properties

The thermal characteristics of the PCMs were evaluated using high-pressure capsules in a differential scanning calorimeter from Mettler Toledo (model DSC82, Mississauga, ON, Canada). Ten-milligram samples of each PCM were analyzed. The thermal characteristics of the compounds obtained, on the other hand, were evaluated using a differential scanning calorimeter from PerkinElmer DSC (model DSC6000, Waltham, MA, USA). Five-milligram samples of each compound were used for analysis. Both analyses were carried out in accordance with ASTM standard D3418 [36]. The differential scanning calorimetry analysis made it possible to determine the melting and crystallization temperatures and the latent heat. The analyses were performed using a heating/cooling rate of 10 °C/min in a controlled nitrogen atmosphere.

#### 2.3.4. Thermal Stability

The thermal stability of the MDF residues and the compounds obtained was assessed using a thermogravimetric analyzer from TA Instruments (model Q50, New Castle, DE, USA). Ten-milligram samples of material were analyzed. The analyses were performed using a heating/cooling rate of 10 °C/min in a controlled nitrogen atmosphere. Measurements were taken up to 500 °C. This analysis made it possible to determine the degradation temperatures of the samples.

### *2.4. Statistical Analysis*

To investigate the effect of incorporating PCMs into MDF residues, a two-way analysis of variance (ANOVA) was conducted on the data obtained using the statistical software SPSS version 21 (IBM Corp., Armonk, NY, USA). The significance was determined with $p < 0.05$ for all the conditions evaluated.

## 3. Results

### *3.1. Granulometric and Chemical Analysis of MDF Fibers*

The size distribution of the MDF fibers is shown in Figure 2. The unscreened residue samples contain 7.6% fine particles and have an average fiber size of approximately 1.19 mm, which wis retained by a #14 mesh sieve. This particle size is not observed in the screened residue samples. In the case of the #50 (0.29 mm) mesh sieve, the unscreened residues contain a higher proportion of fine particles (21.5%) than the screened residues (9%) do. In contrast, the screened residue samples contain more fine particles retained by the #60 (0.25 mm) and #70 (0.21 mm) mesh sieves, at 22% and 18%, respectively. Similar proportions of fibers are collected at the bottom of the sieve for the screened and unscreened residues. There is a discernible decrease in particle size in contrast to the fibers utilized to manufacture MDF panels. A larger percentage of MDF fibers is retained by the #50 mesh sieve, as fibers of this size ensure the panel produced has the desired mechanical properties. The residue samples contain a larger proportion of small particles than the panel fiber samples do, as is evidenced by the notable amount of fine material retained at the bottom of the sieve for the residue samples. As the MDF residues become smaller, they are not reused to manufacture new boards. Only a small percentage of screened residues is used as filler for manufacturing MDF panels. However, this reduction in particle size leads to an increase in the specific surface area, which enhances the material's absorption capacity for impregnation. This characteristic proves advantageous when it comes to incorporating PCM. Note, only the unscreened residues are used for the following characterizations and analyses. This approach is adopted due to the predominant accumulation of these underutilized materials.

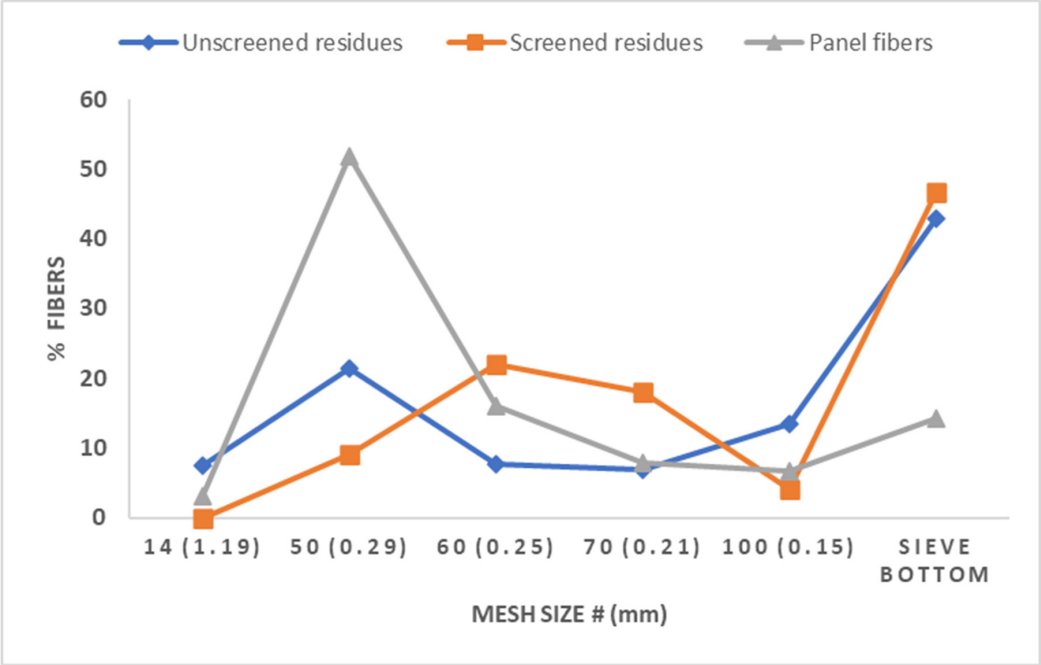



**Figure 2.** Size distribution of fibers used for MDF panel production and of MDF residues.

The chemical composition of the MDF residues is shown in Table 1. They contain 57.6% holocellulose, of which 37.7% is cellulose. The cellulose content value obtained in this study is lower than the value reported by Ariete Merino [37], who states Chilean Pinus radiata wood contains 53.7% cellulose. However, it is similar to the value reported by Cruz et al. [38], who reported 38.4% cellulose. The hemicellulose content value obtained in this study is 19.8%, which is similar to the value reported by Singh et al. [39] (20.1%). The residues were found to contain 39.9% lignin, more specifically 34.0% insoluble lignin and 5.9% soluble lignin. These values are significantly higher than those reported by Santos et al. [40]. The presence of residual UF adhesive in the anatomical features of the MDF residue fibers may contribute to this difference. Since the UF adhesive was not removed before chemical analysis, the UF particles add to the overall oven-dry mass of the sample and lead to an overestimation of the real lignin content. This study aimed to assess the impregnation of residues that had not undergone any prior modification. Since the MDF residues had this characteristic, the percentage of lignin in neat Pinus radiata fibers used for MDF panel production was also determined. The percentage of lignin obtained was 26.8%, more specifically 26.2% insoluble lignin and 0.6% soluble lignin. These values are lower than those obtained for the residues, which confirms the reported values may be related to the presence of adhesive particles. The lignin values obtained for the panel fibers are similar to those reported by Ariete Merino [37] and Singh et al. [39]. The MDF residue samples were found to contain approximately 1.1% extractives and 1% ash.

**Table 1.** Chemical composition of MDF fibers.

| Chemical Component | MDF Residues | Panel Fibers | Cruz et al. [38] | Santos et al. [40] | Reyes et al. [41] | Singh et al. [39] | Ariete Merino [37] |
|---|---|---|---|---|---|---|---|
| Holocellulose (%) | 57.6 | 69.6 | 67.9 | 65.0 | 67.2 | 65.6 | 70.1 |
| Cellulose (%) | 37.7 | 49.7 | 38.4 | 43.8 | 41.2 | 45.5 | 53.7 |
| Hemicellulose (%) | 19.8 | 19.9 | 29.5 | 21.2 | 26.0 | 20.1 | 16.4 |
| Lignin (%) | 39.9 | 26.8 | 29.3 | 32.0 | 27.8 | 27.4 | 27.1 |
| Insoluble lignin (%) | 34.0 | 26.2 | - | 26.6 | - | 26.7 | - |
| Soluble lignin (%) | 5.9 | 0.6 | - | 5.4 | - | 0.7 | - |
| Extractives (%) | 1.1 | 2.3 | 2.1 | 3.2 | 1.9 | 0.5 | 1.3 |
| Ash (%) | 1.0 | 0.6 | - | - | - | - | - |

The higher the percentage of lignin in the residues, the fewer the number of voids that can be filled with PCM. However, the high lignin content of the residues used in this study is attributable to adhesive particles, and they do not hinder PCM impregnation. The PCM impregnation rates arrived at in this study cannot be compared with the values reported in other studies that show removing lignin in wood increases the PCM retention percentage [25,27]. This study demonstrates it is possible to impregnate residues containing adhesive with different PCMs.

### *3.2. Morphological Characterization*

The SEM images of the MDF residues and the compounds formed are shown in Figure 3. The morphology of the residues (R) is depicted in Figure 3A. The residue fibers exhibit a predominantly cylindrical shape with well-defined lumens and a rough surface. Since the residues are a byproduct of molding production, their fibers appear to be cut and broken. The fibers used to manufacture MDF panels are typically 3–3.5 mm long, significantly longer than the average length of 1.4 mm observed for the residue fibers studied. The residue fibers have an average width of 40.6 µm, similar to the fibers' original width before panel conversion. Figure 3B–D display the morphology of the residue fibers impregnated with the different PCMs. In contrast to the (unimpregnated) residue fibers, the surfaces of the impregnated fibers appear smoother. This suggests the three PCMs were absorbed by the cell walls and, therefore, filled the available porous spaces and formed a shape-stabilized compound. No differences were observed between the surfaces of the fibers of the three compounds. They all have one factor in common: the PCMs seem to be absorbed by the porous fibers' cell walls.

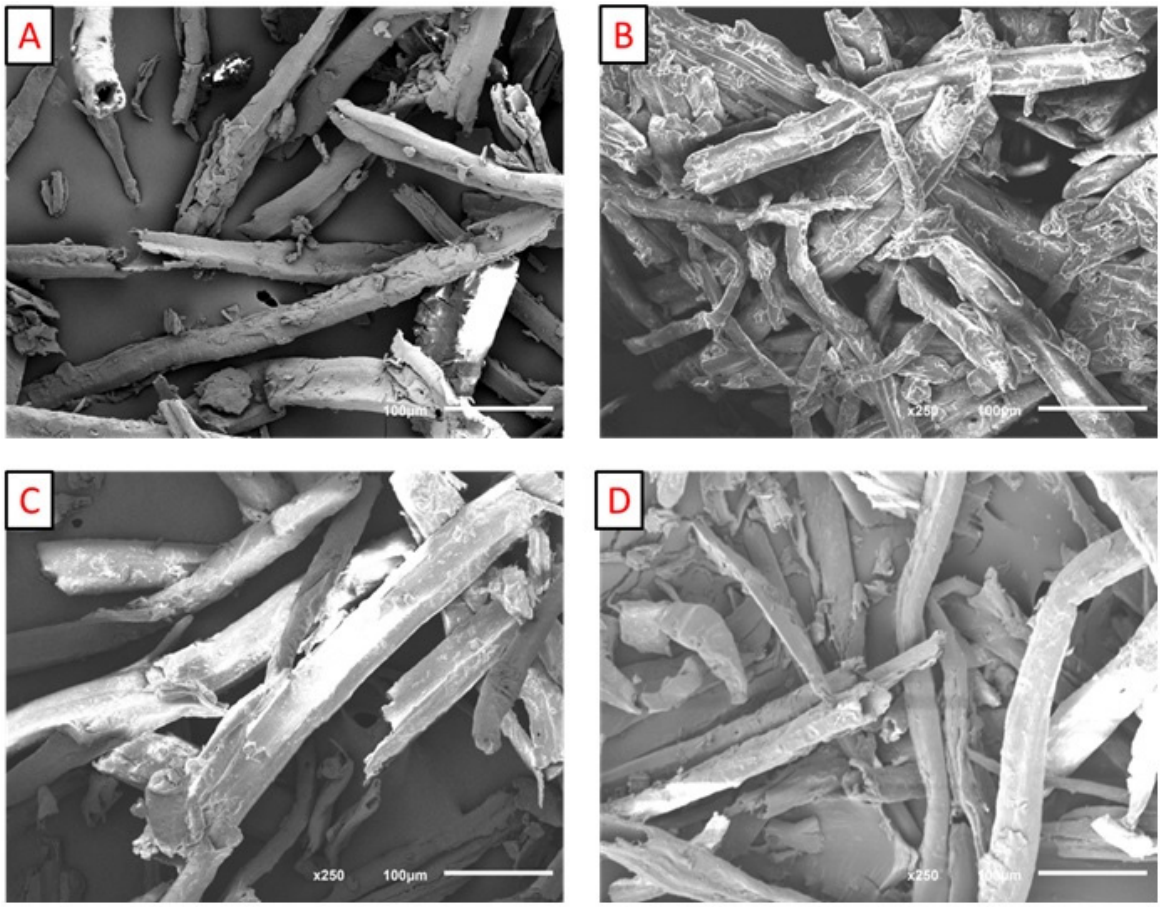



**Figure 3.** SEM images of the MDF residues and the compounds formed. (**A**) MDF residues; (**B**) R+PCM1; (**C**) R+PCM2; (**D**) R+PCM3.

### 3.3. Chemical Structure

The FTIR spectra of the residues, the PCMs, and the compounds formed are presented in Figure 4. Figure 4A shows the spectra of the MDF residues, the bio-based PCM (PCM1), and the compound formed by combining the two (R+PCM1). The residues exhibit major absorption bands at 3397 $cm^{-1}$, which correspond to the stretching of the O-H groups involved in intermolecular and intramolecular hydrogen bonds. Then, at 2920 $cm^{-1}$, the peak corresponds to the stretching of the C-H groups, specifically the methylene groups present in the material's cellulose [42]. Finally, the 1054 $cm^{-1}$ peak corresponds to the stretching of the C-O groups associated with the material's hemicellulose [39]. PCM1 exhibits peaks at 2926 $cm^{-1}$ and 2857 $cm^{-1}$ corresponding to the stretching of the aliphatic C-H and $CH_2$ groups. The absorption peak characteristic of the C=O functional group in fatty acid esters is observed at 1739 $cm^{-1}$, while the presence of carbonyl associated with inorganic carbonate is reflected at 1460 $cm^{-1}$. Additionally, the band at 1172 $cm^{-1}$ is attributed to the stretching of the C-O groups. Comparing the spectra of the residues and PCM1 with the spectrum of the compound R+PCM1 (Figure 4A) makes it possible to identify the peaks characteristic of each component. However, Figure 4B demonstrates the interaction of the compound's components results in variations in the intensity of the characteristic peaks.

This suggests that despite the same functional groups being present, their quantities may differ, as shown by the height of the peaks, without altering the chemical composition of the compound. Furthermore, no new peaks were observed in R+PCM1's spectrum, which indicates no chemical reaction occurred between the residues and PCM1.

Figure 4C displays the FTIR spectra of the MDF residues (the same ones analyzed previously), PCM2 (a petroleum-derived paraffin), and the compound formed by combining the two (R+PCM2). The characteristic peaks observed in PCM2's spectrum at 2922 $cm^{-1}$ and 2855 $cm^{-1}$ are associated with the stretching vibrations of the C-H groups in methylene. The peak at 1464 $cm^{-1}$ corresponds to the bending of the C-H chain in the methyl/methylene groups [43]. Additionally, the peak observed at 721 $cm^{-1}$ is associated with the oscillation of the methylene groups [44]. Similar observations can be made for PCM3, whose spectrum is shown in Figure 4E.

When the spectra of the residues and PCM2 are compared with the spectrum of the compound R+PCM2, a similar trend is observed as is noted above for R+PCM1. There are no new peaks indicating a change in the chemical composition of the compound. However, the same cannot be said for the compound R+PCM3. Its spectrum (see Figure 4E,F) suggests little or no PCM3 was incorporated into the residues' anatomical features. The peaks observed at 2927 $cm^{-1}$ and 2860 $cm^{-1}$ in PCM3's spectrum are absent in R+PCM3's spectrum. As for the peaks observed at 1464 $cm^{-1}$ and 716 $cm^{-1}$ in PCM3's spectrum, they may or may not be present in R+PCM3's spectrum as they overlap with the residues' characteristic peaks.

The FTIR spectrometry results indicate the feasibility of impregnating MDF residues with PCMs and reveal a high degree of compatibility. The physical bonding occurring between each PCM and the residues prevents the formation of new compounds by chemical reaction. The initial chemical composition of both components is maintained and improves the compound's heat storage capacity. This novel approach establishes MDF residues as a promising material for heat storage applications.

### 3.4. Thermal Properties

Table 2 shows the characterization results of the PCMs considered. PCM1 exhibits the highest latent heat of fusion, at 184.3 $J \cdot g^{-1}$. Its fusion temperature is 15.3 °C, and its crystallization temperature is 8.2 °C. PCM2 and PCM3 exhibit similar thermal properties and have lower latent heat values than PCM1.

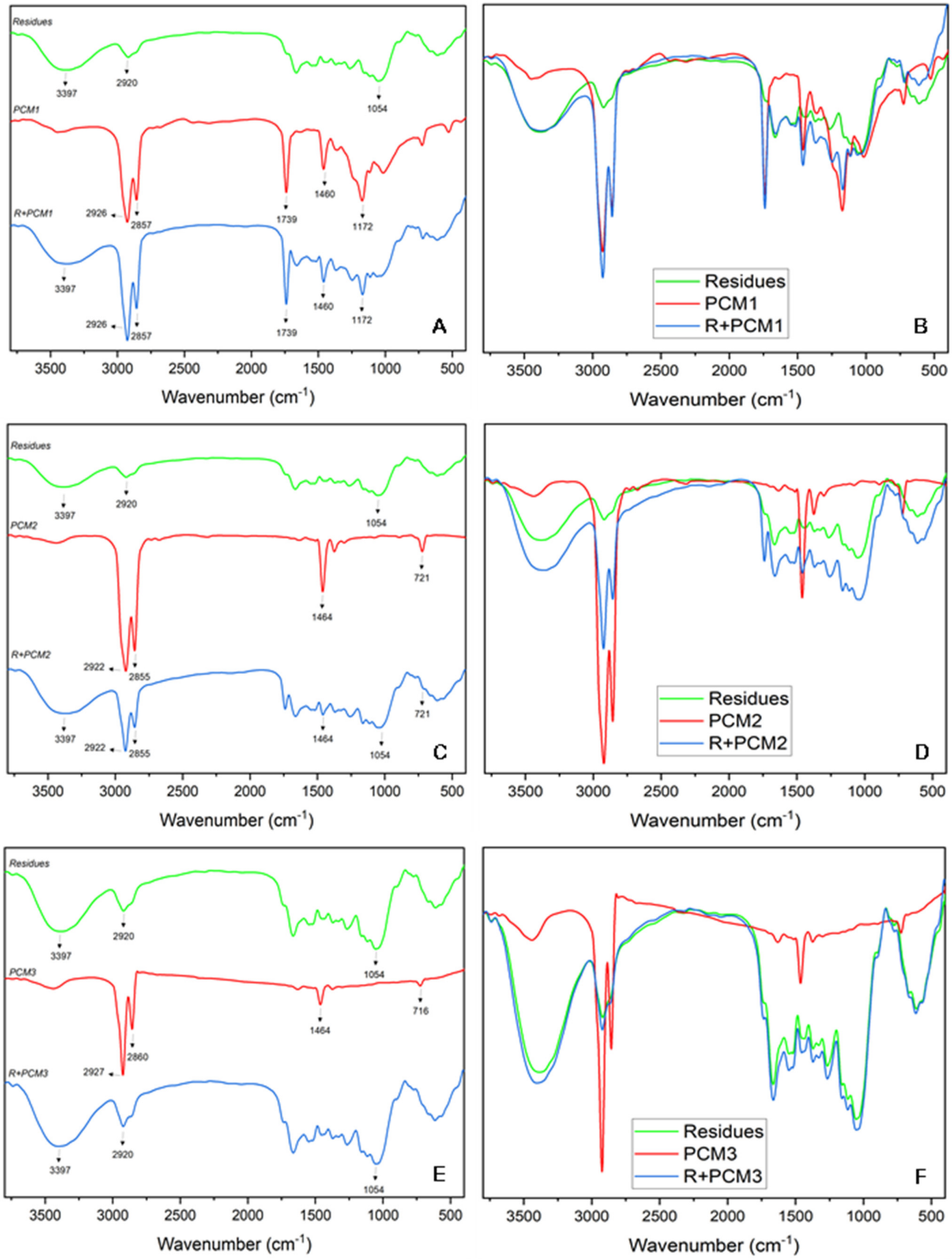



**Figure 4.** FTIR spectra of the MDF residues (R), the PCMs (1,2 and 3), and the corresponding compounds formed. (**A**) Spectra of R, PCM1, and R+PCM1; (**B**) comparative analysis of the spectra in (**A**); (**C**) spectra of R, PCM2, and R+PCM2; (**D**) comparative analysis of the spectra in (**C**); (**E**) spectra of R, PCM3, and R+PCM3; (**F**) comparative analysis of the spectra in (**D**).

**Table 2.** Thermal properties of the PCMs used.

| PCM | Fusion Temperature ($T_f$) | Latent Heat of Fusion ($\Delta H_f$) | Crystallization Temperature ($T_c$) | Latent Heat of Crystallization ($\Delta H_c$) |
|---|---|---|---|---|
| | °C | J g$^{-1}$ | °C | J g$^{-1}$ |
| PCM1 | 15.3 | 184.3 | 8.2 | 177.0 |
| PCM2 | 13.3 | 143.6 | 7.2 | 137.2 |
| PCM3 | 13.9 | 141.9 | 7.0 | 124.5 |

Table 3 presents the thermal properties of the compounds obtained. As expected, the compounds have lower latent heat of fusion values than the pure PCMs have. This is primarily due to the absence of phase change in the MDF residues. The compound R+PCM1 has the highest latent heat of fusion, at 57.8 J·g$^{-1}$. Its fusion temperature is similar to that of PCM1. Although the MDF residues contain adhesive particles, it is possible to incorporate PCM in their fibers' anatomical features.

**Table 3.** Thermal properties of the shape-stabilized compounds obtained.

| Compound | Fusion Temperature ($T_f$) | Latent Heat of Fusion ($\Delta H_f$) |
|---|---|---|
| | °C | J g$^{-1}$ |
| R+PCM1 | 15.8 | 57.8 |
| R+PCM2 | 24.5 | 19.3 |
| R+PCM3 | 28.2 | 0.5 |

The latent heat of fusion value obtained for R+PCM1 in this study is comparable to the values reported by Ma et al. [27]. Their research revealed wood had a latent heat of fusion value of 71.8 J·g$^{-1}$, while for delignified wood, this was 94.4 J·g$^{-1}$, after impregnation with a eutectic mixture of capric and palmitic acids. The values obtained for compound R+PCM2 were comparable to those obtained by Barreneche et al. [45], who impregnated wood with similar paraffin waxes and achieved a latent heat of fusion value of 20.6 J·g$^{-1}$. Our study is the only one thus far to have incorporated a PCM in MDF fiber residues containing UF adhesive particles. Therefore, the similarity of the results obtained in this study for residues containing adhesive particles and those reported by Ma et al. and Barreneche et al. (for samples without adhesive), indicates the adhesive's presence does not influence PCM incorporation. On the other hand, it is worth mentioning, the latent heat of fusion value obtained in this study for R+PCM3 is very low, which may be attributable to a lack of PCM absorption in the wood anatomical features of the MDF residues.

The encapsulation ratio of PCM in the residues' fibers was calculated from the latent heat of fusion values (determined by DSC analysis) using Equation (1) [46]:

$$R = \frac{\Delta H_{f,R+PCM}}{\Delta H_{f,PCM}} * 100\% \quad (1)$$

where $R$ is the encapsulation ratio, and $\Delta H_{f,R+PCM}$ and $\Delta H_{f,PCM}$ are the latent heat of fusion of the compound and the PCM, respectively. The results indicate PCM1's encapsulation ratio in R+PCM1 was 31.4%, PCM2's ratio in R+PCM2 was 13.4%, and PCM3's ratio in R+PCM3 was 0.4%. Therefore, the greater incorporation of the bio-based PCM (PCM1) in the wood anatomical features of the MDF residues leads to the compound R+PCM1 being able to store more thermal energy. These results confirm this compound's suitability as a thermal storage material for construction applications.

### *3.5. Thermal Stability*

Figure 5A shows the thermogravimetric (TG) curves of the MDF residues and the compounds obtained, to provide information about their thermal stability and changes in their

composition. Moreover, Figure 5B shows the corresponding derivative thermogravimetric (DTG) curves, which represent the rate of mass change as a function of temperature. The degradation process of the MDF residues and the compound R+PCM2 is characterized by three distinct steps, as evidenced by the three peaks observed in their DTG curves in Figure 5B. In the first stage, the MDF residues begin to degrade at 33 °C, with a peak degradation temperature of 41.3 °C. The second and third degradation stages begin at 81.6 °C and 363.5 °C and reach maximum degradation temperatures of 326.4 °C and 562 °C, respectively (Figure 5B). The three stages' corresponding weight loss percentages are 3.4%, 60.9%, and 34.1% and are attributable to the water, cellulose, and lignin present in the residues, respectively [47,48].

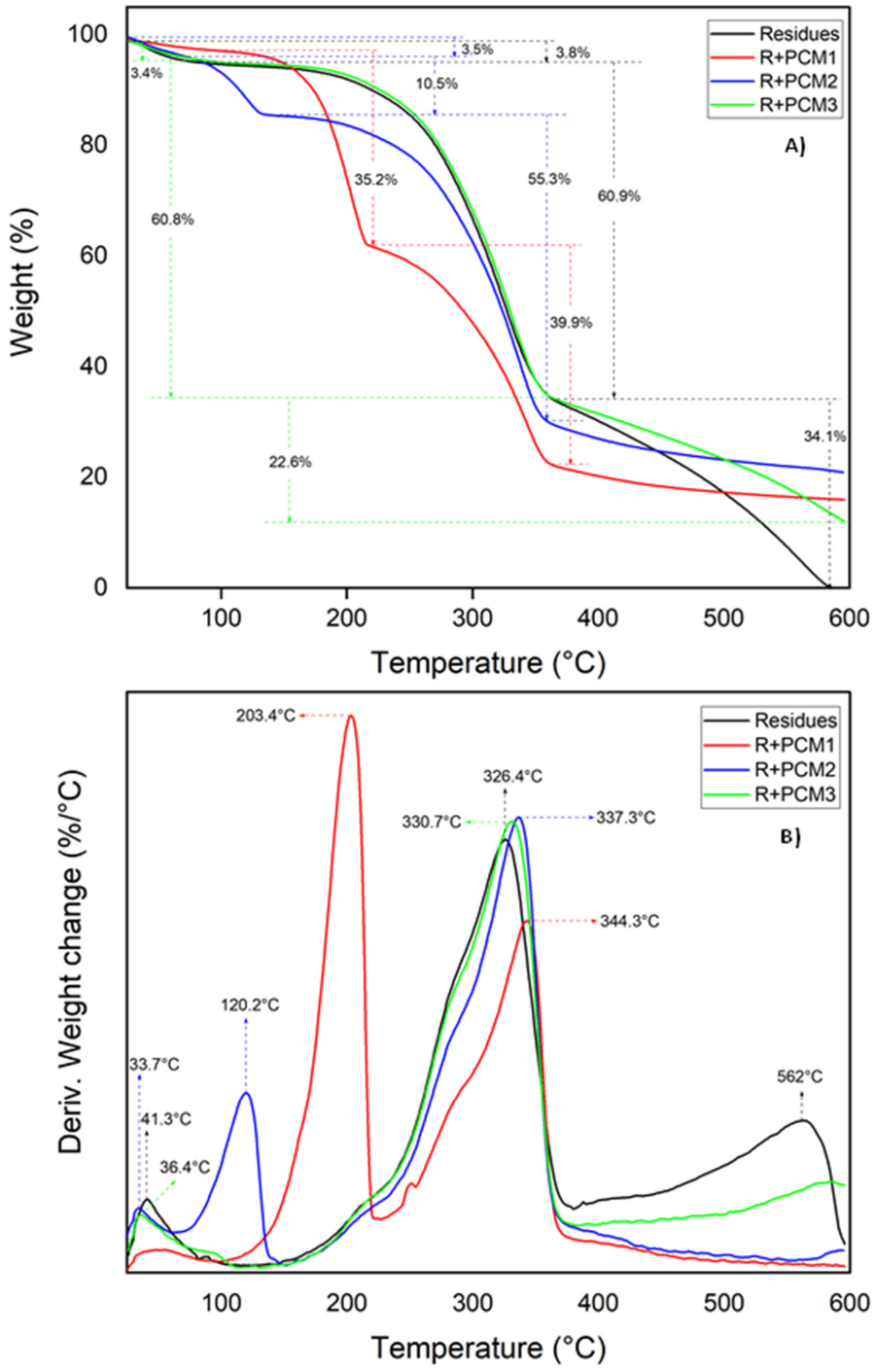



**Figure 5.** (**A**) TG and (**B**) DTG curves of the MDF residues and the compounds obtained.

As for compound R+PCM2, its first degradation step has a maximum degradation temperature of 33.7 °C and results in a 3.5% loss in weight. Its second and third degradation steps have maximum degradation temperatures of 120.2 °C and 337.3 °C, with corresponding weight loss percentages of 10.5% and 55.3%, respectively. R+PCM2′s first and second degradation steps are attributable to water loss, and the third to cellulose [46]. Compounds R+PCM1 and R+PCM3, on the other hand, undergo degradation in two steps, as evidenced by the two peaks in their DTG curves in Figure 5B. Compound R+PCM1′s first degradation step has a maximum degradation temperature of 203.4 °C and results in a 35.2% loss in weight. Its second degradation step has a maximum temperature of 344.3 °C and results in a 39.9% loss in weight. For compound R+PCM3, its first degradation stage reaches a maximum temperature of 36.4 °C and results in a 3.4% loss in weight. Its second degradation step has a maximum temperature of 330.7 °C and results in a 60.8% loss in weight.

These thermal stability results highlight how the degradation behavior of the MDF residues and the compounds differ and emphasize the effect impregnation with PCMs has on their thermal properties.

Overall, the compounds exhibit good thermal stability. Notably, R+PCM1 has a significantly higher degradation onset temperature of over 200 °C, whereas the compounds formulated with petroleum-derived PCMs (R+PCM2 and R+PCM3) begin degrading at temperatures below 40 °C. This indicates the compound formulated using the bio-based PCM exhibits superior thermal performance.

### *3.6. Absorption of PCM by MDF Residues*

The type of PCM, as well as the time and temperature, significantly affected the percentage of PCM absorbed by the impregnated MDF residues. The interaction of these factors also had a significant effect. The residues impregnated with PCM1 had higher absorption capacities than those impregnated with the other PCMs. The best absorption performance (142.8%) was obtained with the following time and temperature parameters: 20 min and 60 °C. The petroleum-derived PCMs performed considerably less well than the bio-based PCM, with absorption values below 50%.

## 4. Conclusions

The study of MDF residues revealed they are composed of fibers smaller in length than the fibers typically used to produce MDF panels. Nevertheless, these residues can be effectively impregnated with different phase change materials (PCMs) to improve their thermal storage capacity. Challenges were encountered when chemically characterizing the residues considered because the presence of adhesive particles in the residues made it difficult to accurately determine the amount of lignin present. The values obtained deviated from those reported in existing studies on *Pinus radiata* wood. The impregnation process used for the MDF residues was successful and led to the formation of a physical bond between the fibers and the PCMs. The absence of chemical reactions between the constituents of the residues and the PCMs was confirmed by FTIR spectrometry. Of the compounds obtained, R+PCM1 demonstrated the best thermal properties, with a latent heat of fusion of 57.8 $J \cdot g^{-1}$ and a fusion temperature similar to PCM1's. In addition, it had both the highest encapsulation ratio and the highest absorption capacity of the compounds evaluated. In general, all the compounds demonstrated commendable thermal stability.

The findings of this study demonstrate the feasibility of using MDF residues as an alternative source of raw material to produce compounds capable of storing thermal energy. One potential application of these compounds is in construction, to build walls, ceilings, and partition systems with enhanced passive heat storage capacity. The compounds developed could be utilized in the manufacturing of panels, which could function as integral wall components. They could regulate the temperature inside buildings by absorbing and releasing thermal energy, thereby improving indoor thermal comfort. Therefore, this presents

an opportunity to valorize MDF residues generated in the wood-based panel industry and provides a solution to alleviate the physical storage challenges panel manufacturers face.

Further research should focus on optimizing the impregnation process and investigating potential thermal energy storage applications for these types of compounds. The compounds obtained can be used in the development of novel materials. By making use of residue resources and adopting sustainable practices, the wood-based panel industry can contribute to a more circular and environmentally conscious approach to material utilization.

**Author Contributions:** Conceptualization, G.E.R. and C.B.Á.; methodology, G.E.R.; formal analysis, G.E.R. and C.B.Á.; investigation, G.E.R.; resources, C.B.Á.; data curation, G.E.R.; writing—original draft preparation, G.E.R.; writing—review and editing, G.E.R., C.B.Á., R.R. and A.C.; visualization, G.E.R. and C.B.Á.; supervision, C.B.Á. and A.C.; project administration, G.E.R. and C.B.Á.; funding acquisition, C.B.Á. All authors have read and agreed to the published version of the manuscript.

**Funding:** This research was funded by an internal Universidad del Bío Bío (UBB) project on innovation and development (Code I+D 22-48).

**Institutional Review Board Statement:** Not applicable.

**Data Availability Statement:** The data presented in this article are available upon reasonable request from the corresponding authors.

**Acknowledgments:** The authors would like to acknowledge UBB's Center for Biomaterials and Nanotechnology for allowing them to use its laboratories and equipment. The authors would also like to thank UBB's Doctoral Scholarship and Research Grant and the team of the internal UBB project on innovation and development (Code: I+D 22-48).

**Conflicts of Interest:** The authors declare no conflict of interest.

## References

1. Gysling Caselli, J.; Soto Aguirre, D. *Industria Forestal Primaria En Chile. Período 2006–2015*; INFOR: Santiago, Chile, 2016.
2. Soto Aguirre, D.; Gysling Caselli, J.; Pardo, V.E. *La Industria de Tableros y Chapas 2022*; INFOR: Santiago, Chile, 2022.
3. Gysling Caselli, J.; Bañados, M.J.C. *Subproductos Madereros de La Industria Del Aserrío 2022*; INFOR: Santiago, Chile, 2022.
4. Giannotas, G.; Kamperidou, V.; Barboutis, I. Tree Bark Utilization in Insulating Bio-Aggregates: A Review. *Biofuels Bioprod. Biorefin.* **2021**, *15*, 1989–1999. [CrossRef]
5. Lin, Y.; Alva, G.; Fang, G. Review on Thermal Performances and Applications of Thermal Energy Storage Systems with Inorganic Phase Change Materials. *Energy* **2018**, *165*, 685–708. [CrossRef]
6. Liu, L.; Su, D.; Tang, Y.; Fang, G. Thermal Conductivity Enhancement of Phase Change Materials for Thermal Energy Storage: A Review. *Renew. Sustain. Energy Rev.* **2016**, *62*, 305–317. [CrossRef]
7. Vennapusa, J.R.; Konala, A.; Dixit, P.; Chattopadhyay, S. Caprylic Acid Based PCM Composite with Potential for Thermal Buffering and Packaging Applications. *Mater. Chem. Phys.* **2020**, *253*, 123453. [CrossRef]
8. Khan, Z.; Khan, Z.; Ghafoor, A. A Review of Performance Enhancement of PCM Based Latent Heat Storage System within the Context of Materials, Thermal Stability and Compatibility. *Energy Convers. Manag.* **2016**, *115*, 132–158. [CrossRef]
9. Jeong, S.G.; Jeon, J.; Seo, J.; Lee, J.H.; Kim, S. Performance Evaluation of the Microencapsulated PCM for Wood-Based Flooring Application. *Energy Convers. Manag.* **2012**, *64*, 516–521. [CrossRef]
10. Safari, A.; Saidur, R.; Sulaiman, F.A.; Xu, Y.; Dong, J. A Review on Supercooling of Phase Change Materials in Thermal Energy Storage Systems. *Renew. Sustain. Energy Rev.* **2017**, *70*, 905–919. [CrossRef]
11. Kośny, J. *PCM-Enhanced Building Components. An Application of Phase Change Materials in Building Envelopes and Internal Structures*; Springer: Cham, Switzerland, 2015.
12. Rathod, M.K.; Banerjee, J. Thermal Stability of Phase Change Materials Used in Latent Heat Energy Storage Systems: A Review. *Renew. Sustain. Energy Rev.* **2013**, *18*, 246–258. [CrossRef]
13. Kant, K.; Shukla, A.; Sharma, A. Ternary Mixture of Fatty Acids as Phase Change Materials for Thermal Energy Storage Applications. *Energy Rep.* **2016**, *2*, 274–279. [CrossRef]
14. Yaras, A.; Ustaoglu, A.; Gencel, O.; Sarı, A.; Hekimoğlu, G.; Sutcu, M.; Erdogmus, E.; Kaplan, G.; Bayraktar, O.Y. Characteristics, Energy Saving and Carbon Emission Reduction Potential of Gypsum Wallboard Containing Phase Change Material. *J. Energy Storage* **2022**, *55*, 105685. [CrossRef]
15. Kumar, N.; Rathore, P.K.S.; Kumar Pal, A. Experimental Investigation of Composite Gypsum Board Integrated with Phase Change Material for Improved Thermal Energy Storage. *Mater. Today Proc.* **2023**, *80*, 1573–1578. [CrossRef]

16. Bake, M.; Shukla, A.; Liu, S. Development of Gypsum Plasterboard Embodied with Microencapsulated Phase Change Material for Energy Efficient Buildings. *Mater. Sci. Energy Technol.* **2021**, *4*, 166–176. [CrossRef]
17. Chen, C.; Wang, X.; Ma, F.; Wang, Y.; Jiu, S.; Chen, Y. Preparation and Characterization of Modified Activated Carbon-Based Shape Stabilized Eutectic Phase Change Materials for Gypsum Composites Application. *Constr. Build. Mater.* **2023**, *369*, 130551. [CrossRef]
18. Hamdaoui, S.; Bouchikhi, A.; Azouggagh, M.; Akour, M.; Ait Msaad, A.; Mahdaoui, M. Building Hollow Clay Bricks Embedding Phase Change Material: Thermal Behavior Analysis under Hot Climate. *Sol. Energy* **2022**, *237*, 122–134. [CrossRef]
19. Gupta, M.K.; Rathore, P.K.S.; Kumar, R.; Gupta, N.K. Experimental Analysis of Clay Bricks Incorporated with Phase Change Material for Enhanced Thermal Energy Storage in Buildings. *J. Energy Storage* **2023**, *64*, 107248. [CrossRef]
20. Chihab, Y.; Bouferra, R.; Garoum, M.; Essaleh, M.; Laaroussi, N. Thermal Inertia and Energy Efficiency Enhancements of Hollow Clay Bricks Integrated with Phase Change Materials. *J. Build. Eng.* **2022**, *53*, 104569. [CrossRef]
21. Wang, Y.; Li, Q.; Miao, W.; Su, Y.; He, X.; Strnadel, B. The Thermal Performances of Cement-Based Materials with Different Types of Microencapsulated Phase Change Materials. *Constr. Build. Mater.* **2022**, *345*, 128388. [CrossRef]
22. Gbekou, F.K.; Benzarti, K.; Boudenne, A.; Eddhahak, A.; Duc, M. Mechanical and Thermophysical Properties of Cement Mortars Including Bio-Based Microencapsulated Phase Change Materials. *Constr. Build. Mater.* **2022**, *352*, 129056. [CrossRef]
23. Kumar, G.N.; Ram, V.V.; Parameshwaran, R. Thermal and Structural Properties of Cement Mortar Embedded with Hybrid Nanocomposite Based Phase Change Nanocapsules for Building Application. *Constr. Build. Mater.* **2023**, *385*, 131481. [CrossRef]
24. Baccega, E.; Bottarelli, M.; Cesari, S. Addition of Granular Phase Change Materials (PCMs) and Graphene to a Cement-Based Mortar to Improve Its Thermal Performances. *Appl. Therm. Eng.* **2023**, *229*, 120582. [CrossRef]
25. Meng, Y.; Majoinen, J.; Zhao, B.; Rojas, O.J. Form-Stable Phase Change Materials from Mesoporous Balsa after Selective Removal of Lignin. *Compos. Part B Eng.* **2020**, *199*, 108296. [CrossRef]
26. Frazzica, A.; Brancato, V.; Palomba, V.; La Rosa, D.; Grungo, F.; Calabrese, L.; Proverbio, E. Thermal Performance of Hybrid Cement Mortar-PCMs for Warm Climates Application. *Sol. Energy Mater. Sol. Cells* **2019**, *193*, 270–280. [CrossRef]
27. Ma, L.; Wang, Q.; Li, L. Delignified Wood/Capric Acid-Palmitic Acid Mixture Stable-Form Phase Change Material for Thermal Storage. *Sol. Energy Mater. Sol. Cells* **2019**, *194*, 215–221. [CrossRef]
28. Cheng, L.; Feng, J. Form-Stable Phase Change Materials Based on Delignified Wood Flour for Thermal Management of Buildings. *Compos. Part A Appl. Sci. Manuf.* **2020**, *129*, 105690. [CrossRef]
29. Jiang, L.; Lei, Y.; Liu, Q.; Wang, Y.; Zhao, Y.; Lei, J. Facile Preparation of Polyethylene Glycol/Wood-Flour Composites as Form-Stable Phase Change Materials for Thermal Energy Storage. *J. Therm. Anal. Calorim.* **2020**, *139*, 137–146. [CrossRef]
30. Sarı, A.; Hekimoglu, G.; Tyagi, V.V. Low Cost and Eco-Friendly Wood Fiber-Based Composite Phase Change Material: Development, Characterization and Lab-Scale Thermoregulation Performance for Thermal Energy Storage. *Energy* **2020**, *195*, 116983. [CrossRef]
31. Liang, J.; Zhimeng, L.; Ye, Y.; Yanjun, W.; Jingxin, L.; Changlin, Z. Fabrication and Characterization of Fatty Acid/Wood-Flour Composites as Novel Form-Stable Phase Change Materials for Thermal Energy Storage. *Energy Build.* **2018**, *171*, 88–99. [CrossRef]
32. *TAPPI T280 Wd-08*; Acetone Extractives of Wood and Pulp. TAPPI Press: Atlanta, GA, USA, 2015.
33. *TAPPI T9 Wd-75*; Hollocelulose in Wood. TAPPI Press: Atlanta, GA, USA, 2015.
34. *TAPPI T222 Om-11*; Acid-Insoluble Lignin in Wood and Pulp. TAPPI Press: Atlanta, GA, USA, 2015.
35. *TAPPI T211 Om-12*; Ash in Wood, Pulp Paper and Paperboard: Combustion at 525 °C. TAPPI Press: Atlanta, GA, USA, 2015.
36. *ASTM D3418-12*; Standard Test Method for Transition Temperatures and Enthalpies of Fusion and Crystallization of Polymers by Differential Scanning Calorimetry. ASTM International: West Conshohocken, PA, USA, 2012. [CrossRef]
37. Ariete Merino, N.A. *Caracterización de Madera de Pinus Radiata D. Don Sometido a Un Proceso de Modificación Térmica Usando Un Ambiente de Inmersión*; Universidad Austral de Chile: Valdivia, Chile, 2010.
38. Cruz, N.; Bustos, C.; Aguayo, M.G.; Cloutier, A.; Castillo, R. Impact of the Chemical Composition of Pinus Radiata Wood on Its Physical and Mechanical Properties Following Thermo-Hygromechanical Densification. *BioResources* **2018**, *13*, 2268–2282. [CrossRef]
39. Singh, T.; Singh, A.P.; Hussain, I.; Hall, P. Chemical Characterisation and Durability Assessment of Torrefied Radiata Pine (Pinus Radiata) Wood Chips. *Int. Biodeterior. Biodegrad.* **2013**, *85*, 347–353. [CrossRef]
40. Santos, T.M.; Alonso, M.V.; Oliet, M.; Domínguez, J.C.; Rigual, V.; Rodriguez, F. Effect of Autohydrolysis on Pinus Radiata Wood for Hemicellulose Extraction. *Carbohydr. Polym.* **2018**, *194*, 285–293. [CrossRef]
41. Reyes, P.; Mendonça, R.T.; Aguayo, M.G.; Rodríguez, J.; Vega, B.; Fardim, P. Extração e Caracterização de Hemiceluloses de Pinus Radiata e Sua Viabilidade Para a Produção de Bioetanol. *Rev. Arvore* **2013**, *37*, 175–180. [CrossRef]
42. Md Salim, R.; Asik, J.; Sarjadi, M.S. Chemical Functional Groups of Extractives, Cellulose and Lignin Extracted from Native Leucaena Leucocephala Bark. *Wood Sci. Technol.* **2021**, *55*, 295–313. [CrossRef]
43. Xia, X.; Shi, R.; Huang, J.; Li, Y.; Zuo, Y.; Li, J. Development of a Phase Change Microcapsule to Reduce the Setting Temperature of PMMA Bone Cement. *J. Appl. Biomater. Funct. Mater.* **2020**, 18. [CrossRef] [PubMed]
44. Memon, S.A.; Liao, W.; Yang, S.; Cui, H.; Shah, S.F.A. Development of Composite PCMs by Incorporation of Paraffin into Various Building Materials. *Materials* **2015**, *8*, 499–518. [CrossRef] [PubMed]
45. Barreneche, C.; Vecstaudza, J.; Bajare, D.; Fernandez, A.I. PCM/Wood Composite to Store Thermal Energy in Passive Building Envelopes. *IOP Conf. Ser. Mater. Sci. Eng.* **2017**, *251*, 19–23. [CrossRef]

46. Salunkhe, P.B.; Shembekar, P.S. A Review on Effect of Phase Change Material Encapsulation on the Thermal Performance of a System. *Renew. Sustain. Energy Rev.* **2012**, *16*, 5603–5616. [CrossRef]
47. Morán, J.I.; Alvarez, V.A.; Cyras, V.P.; Vázquez, A. Extraction of Cellulose and Preparation of Nanocellulose from Sisal Fibers. *Cellulose* **2008**, *15*, 149–159. [CrossRef]
48. Alvarado Flores, J.J.; Rutiaga Quiñones, J.G. Estudio de Cinética En Procesos Termogravimétricos de Materiales Lignocelulósicos. *Maderas Cienc. Tecnol.* **2018**, *20*, 221–238. [CrossRef]

**Disclaimer/Publisher's Note:** The statements, opinions and data contained in all publications are solely those of the individual author(s) and contributor(s) and not of MDPI and/or the editor(s). MDPI and/or the editor(s) disclaim responsibility for any injury to people or property resulting from any ideas, methods, instructions or products referred to in the content.